

## The quantum transition state wavepacket method

John C. Light and Dong Hui Zhang<sup>†</sup>

Department of Chemistry and The James Franck Institute, The University of Chicago,  
Chicago, IL 60637, USA

---

The accurate calculation of thermal rate constants for reactions in the gas phase often requires both accurate potential energy surfaces (PESs) and the use of quantum mechanics, particularly in the case of light atom (H) transfers in reactions with activation energy barriers between reactants and products. The thermal rate constant  $k(T)$  can be calculated directly or as a thermal average over the cumulative reaction probability  $N(E)$ . Both  $k(T)$  and  $N(E)$  can be calculated exactly and directly in terms of flux formulations first presented by Miller *et al.* In this paper we review the recent reformulation of the calculation of  $N(E)$  in terms of the time evolution of transition state wavepackets (TSWPs), which then provides a very effective method for reactions with activation energy barriers. This method requires a single time propagation for each TSWP contributing to the desired thermal rate constant from which the required contributions to  $N(E)$  for all  $E$  can be obtained. We then apply this to the calculation of  $N(E)$  and  $k(T)$  for the interesting four atom reaction  $\text{H}_2(\text{D}_2) + \text{CN} \rightarrow \text{HCN}(\text{DCN}) + \text{H}(\text{D})$ . The system has a metastable well in the PES at the linear CNHH configuration. The results and a discussion of the influence of this secondary TS well are presented.

---

### 1 Introduction

The calculation of thermal rate constants of chemical reactions has long been an important goal of theoretical chemical physicists. For a large class of reactions the reaction rate constants are dominated by the energy required to pass over a barrier on the potential energy surface (PES) leading (approximately) to the Arrhenius form of the rate constants. Classical transition state theory (TST)<sup>1,2</sup> and further developments of variational TSTs<sup>3–9</sup> provide in many cases excellent approximations to thermal rate constants for heavier systems for which the PES is known with reasonable accuracy. However, the dynamical approximations in such TST calculations make it desirable to have a quantum formulation that is both exact and practical. Such calculations will require accurate knowledge of the PES for the full system, at least in the regions of the potential energy barriers separating reactants and products. In addition, the dynamics must be simulated adequately; if light atom transfers are involved in the reactions, the use of quantum dynamics, which includes both discrete energy level effects and quantum tunneling, is highly desirable.

Reaction rate constants can be calculated exactly from thermal averages of exact quantum state-to-state reaction probabilities, *i.e.* from the  $\mathcal{S}$ -matrices obtained from full solutions to the Schrödinger equation at each energy. For reactions with barriers and with relatively sparse reactant and product quantum states, the full  $\mathcal{S}$ -matrix can be calculated. Alternatively the time dependent Schrödinger equation can be solved for

<sup>†</sup> Present address: Department of Computational Science, National University of Singapore, Singapore 119260.

each initial state to obtain the reaction probability as a function of energy from that state. Substantial improvements in the methods used in such initial state selected wavepacket approaches (ISSWP) now permit four atom systems to be solved exactly.<sup>10–15</sup>

However, for reactions with a relatively dense distribution of reactant and product states at the energies of interest, the number of energetically open states contributing to the rate constant will be very large. In these cases, the full  $S$ -matrices or even the initial state selected reaction probabilities may be very difficult to calculate. In addition, the full  $S$ -matrices contain much information on state-to-state probabilities that is averaged to obtain the rate constants. If there is a well defined transition state region with an activation energy barrier, it will be much more efficient to attack the calculation of the rate constant directly or *via* the direct calculation of such averaged quantities as the cumulative reaction probability,  $N(E)$ . In our discussions below we focus on reactions with activation energies for which transition state type theories are most appropriate. The quantum methods discussed are exact for all types of reactions, but their efficiency is greatest for reactions with barriers.

Approaches to the direct quantum calculation of  $k(T)$  and  $N(E)$  were formulated some time ago in very important papers by Miller and co-workers.<sup>16,17</sup> In these formulations dividing surface(s) between reactants and products can be defined as in TST. However, the rate constants or reaction probabilities are given as traces of quantum mechanical (flux) operators. These were discussed by Miller at a Faraday Discussion meeting more than ten years ago,<sup>18</sup> and have been developed and used in a number of applications since that time.<sup>19–27</sup>

The original formulations were quite general permitting the desired rate information to be obtained in a number of exact and formally equivalent ways. The choice between formally equivalent approaches was not obvious, and there have been a variety of actual computational approaches developed with the basic aims of providing rigorous and efficient methods to determine the specific dynamical information of interest. Ideally there should be a small number of intuitive and efficient methods, each tailored for the specific system information desired. Specific methods using the formal definitions of the thermal rate constants,  $k(T)$ , have been developed to calculate it directly. Other approaches can determine the cumulative reaction probability,  $N(E)$ , from which  $k(T)$  can be generated by a Boltzmann average. Yet other approaches can yield more detailed information about reaction from a specified initial state or to a specified final state, by varying the position of the dividing surface(s).

The first calculation of thermal rate constants by these methods for a ‘real’ system, *i.e.* a three-dimensional (3-D) calculation of the reaction of a triatomic system on a realistic surface was that of Park and Light<sup>23</sup> for, naturally, the hydrogen exchange reaction. This was, in a sense, a ‘brute force’ calculation in which the 3-D Hamiltonian was diagonalized on an  $L^2$  basis. The trace was carried out on the basis of the thermal flux operator, determined by Lanczos reduction. The diagonalization permitted the rate constants to be calculated analytically at different temperatures as the time integral of the flux–flux correlation function. The fact that the flux operator is of low rank<sup>22</sup> was utilized to simplify the evaluation of the trace of the correlation function. The validity of this approach was verified by Day and Truhlar<sup>28</sup> and applied by these authors to the O + HD reactions.<sup>29</sup> As a general method, however, the calculation had several flaws: the diagonalization of  $\hat{H}$  becomes prohibitive for larger systems, and, since no absorbing potential was used, accurate results were limited to low temperatures where the effects of reflections from the grid boundaries could be minimized. The obvious utility of absorbing boundary conditions (optical potentials), developed by Neuhauser and Baer<sup>28c</sup> in removing the effect of grid boundaries and permitting the convergence of the time integral of the correlation functions was demonstrated by Brown and Light.<sup>25</sup>

More recently a number of improved approaches have been developed. The ‘transition state probability operator’ approach of Manthe and co-workers<sup>29–31</sup> for the

determination of  $N(E)$  is elegant. The eigenvalues of this operator are probabilities of reaction from each ‘transition state’, and can be obtained by iterative procedures. This approach requires the use of optical potentials, absorbing potentials are also utilized in all subsequent approaches. The advantages of the probability operator approach are that it is variational and relatively few eigenvalues are required [if the dividing transition state surface (TSS) is well placed at the top of an activation energy barrier]. The disadvantages are that the eigenvalues [essentially of the Green operator,  $(H - E - i\epsilon)^{-1}$ ] are not easy to extract by iterative methods and that they must be determined again at each energy. At each energy the number of eigenvalues required is basically the number of transition states contributing to the reaction at that energy.

Two other approaches to the direct calculation of rate constants,<sup>26,32,33</sup> following the approach proposed by Park and Light,<sup>22</sup> are based on the evaluation of the eigenvectors and eigenvalues of the thermal flux operator *via* Lanczos reduction and propagation of these wavepackets. The use of optical potentials makes short time propagations adequate. However, the propagations must be repeated at each temperature at which  $k(T)$  is desired. These approaches have been applied to several important reactions including  $\text{Cl} + \text{H}_2 \rightarrow \text{HCl} + \text{H}$ .<sup>34</sup> Manthe and co-workers have combined this approach with an approximate multi-configuration time dependent Hartree (MCTDH) propagation that is applicable to larger systems.<sup>35,36</sup>

Our TSWP method<sup>37</sup> differs from the above in that the cumulative reaction probabilities at all energies desired are evaluated from a single propagation of each TSWP forward and backward in time, followed by the appropriate Fourier transforms. The  $N(E)$ s so obtained can then be thermally averaged to produce the thermal rate constants at all desired temperatures. This has the advantages that only TSWPs in the energy range of interest are required; the Fourier transforms at each  $E$  must be accumulated only on a dividing (TS) surface; and only one propagation (in  $+t$  and  $-t$ ) is required per transition state. The TSWP approach has been successfully applied to calculate  $N(E)$  for  $J = 0$ <sup>38</sup> and recently  $N(E)$  (summed over all  $J$ )<sup>39</sup> for the prototype four atom reaction  $\text{H}_2 + \text{OH} \rightarrow \text{H}_2\text{O} + \text{H}$ , which provided the first fairly accurate theoretical rate constant for a four atom reaction.

In the following we review the formulation of the TSWP theory and discuss the application to a difficult reaction of interest, the  $\text{H}_2(\text{D}_2) + \text{CN}$  reaction. Since the PES of this system has a transition state in the  $\text{H}-\text{H}-\text{C}-\text{N}$  configuration and a metastable well in the  $\text{C}-\text{N}-\text{H}-\text{H}$  configuration, it is not a simple transition state problem. The location of the dividing surface (the transition state) and the convergence of the cumulative reaction probability with respect to the number of transition states included illustrate the difficulties encountered when reactions with ‘odd’ PESs are considered.

## 2 Theory

### 2.1 TSWP approach

The TSWP approach is similar to the regular time-dependent ISSWP approach to reactive scattering<sup>40,41</sup> except for the initial wavepacket construction. In the ISSWP approach, the initial wavepacket is usually a direct product of a gaussian wavepacket for the translational motion located in the reactant asymptotic region and a specific ( $N - 1$  dimensional) internal state for reactants. In the TSWP approach we first choose a dividing surface  $S_1$  separating the products from reactants preferably located to minimize the value of the density-of-states for the energy region considered. Then initial TSWPs are constructed as the direct products of the ( $N - 1$  dimensional) Hamiltonian eigenstates on the surface

$$H_s |\phi_i\rangle = \epsilon_i |\phi_i\rangle \quad (1)$$

and the flux operator eigenstate,  $|+\rangle$  with positive eigenvalue  $\lambda$ .

$$F|+\rangle = \lambda|+\rangle \quad (2)$$

Thus we have

$$|\phi_i^+\rangle = |\phi_i\rangle|+\rangle \quad (3)$$

The cumulative reaction probability,  $N(E)$ , from the TSWP approach was derived simply from the formulation for  $N(E)$  given by Miller and co-workers,<sup>17</sup>

$$N(E) = 2\pi^2 \text{tr}[\delta(E - H)F_2\delta(E - H)F_1], \quad (4)$$

where  $F_1$  and  $F_2$  are the quantum flux operators at dividing surfaces  $S_1$  and  $S_2$  between reactants and products. The surfaces can be identical, and, for calculation of  $N(E)$  only, would normally both be the transition state surface.

Here the flux operator  $F$  is defined as

$$F = \frac{1}{2\mu} [\delta(q - q_0)\hat{p}_q + \hat{p}_q\delta(q - q_0)] \quad (5)$$

where  $\mu$  is the reduced mass,  $q$  is the coordinate normal to the dividing surface located at  $q = q_0$ , which separates products from reactants, and  $\hat{p}_q$  is the momentum operator conjugate to the coordinate  $q$ . In evaluating the trace, we take advantage of the fact that the flux operator has only two non-zero eigenvalues for one-dimension,<sup>21,22,42</sup>  $\pm\lambda$  with eigenfunctions that are complex conjugates of each other  $|+\rangle = |-\rangle^*$ . We then evaluate the trace in eqn. (4) efficiently in a direct product basis of the flux operator eigenstates, which are highly localized near the dividing surface, and the eigenstates of the  $(N - 1)$  dimensional Hamiltonian on the dividing surface, the transition states.

The microcanonical density operator,  $\delta(E - H)$ , will eliminate contributions to  $N(E)$  from transition states with internal energy much higher than the total energy,  $E$ , thus limiting the number of transition states that must be considered. (Owing to tunneling, of course, the internal states with energy somewhat greater than  $E$  can contribute to the cumulative reaction probability.) Thus by choosing a dividing surface with the lowest density of internal states, we can minimize the number of transition states required to converge  $N(E)$ .

Since  $N(E)$  in eqn. (4) is represented in terms of  $\delta$  function operators, the evaluation is most efficiently carried out utilizing the Fourier transform identity between the energy and time domains. After constructing the initial wavepackets, we propagated them in time, as in the ISSWP approach.

The components of the TSWPs at energy  $E$ ,  $|\psi_i\rangle$ , are calculated on the second dividing surface (at  $x = x_0$ ) as

$$|\psi_i(E)\rangle = \sqrt{\lambda} \int_{-\infty}^{+\infty} e^{i(E-H)t} dt |\phi_i^+\rangle. \quad (6)$$

$$|\phi_i^+\rangle = |\phi_i\rangle|+\rangle \quad \text{with} \quad F|+\rangle = \lambda|+\rangle \quad \text{and} \quad H_{S_1}|\phi_i\rangle = \varepsilon_i|\phi_i\rangle \quad (7)$$

The cumulative reaction probability  $N(E)$  can be computed as

$$N(E) = \sum_i N_i(E) = \sum_i \langle \psi_i | F_2 | \psi_i \rangle = \sum_i \frac{1}{\mu} \text{Im}[\langle \psi_i | \psi_i' \rangle] |_{q=q_0} \quad (8)$$

where the  $|\psi_i'\rangle$  are the derivatives of  $|\psi_i\rangle$  with respect to  $q$ , the coordinate normal to the surface evaluated on the surface  $S_2$  ( $q = q_0$ ). Here  $q$  can be any coordinate as long as the surface of  $F_2$ ,  $q = q_0$  divides the products from reactants.

There are several points to note concerning this compact formulation. First, since the flux operator  $F_2$  exists only at the surface  $S_2$ , the Fourier transform of  $\psi_i$  and its deriv-

ative are required only on that surface, not throughout space. If the surface for  $F_2$  is placed in an asymptotic region, then the flux can be projected onto the asymptotic internal states of the reactants (or products) to obtain the cumulative reaction probabilities (and rate constants) from each initial state, *i.e.* the information obtained from the ISSWP approach. For a single initial state, the ISSWP is to be preferred since only one propagation is required. However, when information for many initial states is desired, and there is a barrier to reaction, then the TSWP approach will converge with many fewer wavepacket propagations.

A perhaps surprising point is that the  $N_i(E)$  above, which are the contributions to  $N(E)$  from each TSWP are not probabilities, *i.e.*  $N_i(E)$  can be negative at some energies and greater than one at others (usually by very small amounts). However,  $N(E)$  itself is a cumulative probability, always greater than zero. Finally, since the TSWPs are determined by the position of the dividing surface  $S_1$  the convergence and behaviour of  $N_i(E)$  vary with the surface. Placement of  $S_1$  in the ‘traditional’ transition state region seems to yield the most rapid convergence with respect to the number of wavepackets required and also seems to produce  $N_i$  values that are ‘almost’ probabilities. We shall see in the application below that because some ‘transition state’ wavepackets for the HHNC reaction start out in the HHNC configuration, the contributions of these wavepackets are zero at low energies, but oscillate with  $E$  at higher energies, and do not behave like probabilities.

### 3 Applications to the $H_2(D_2) + CN$ reaction

In this section, we show the results of the application of the TSWP approach to the  $H_2(D_2) + CN$  reaction. These two reactions have been the subject of active theoretical and experimental research<sup>43–51</sup> because of their practical importance in combustion and atmospheric chemistry. In particular, a new and much improved global PES for the reaction has recently been reported by ter Horst, Schatz and Harding (denoted TSH3).<sup>46</sup> Quasiclassical trajectory calculations,<sup>48</sup> a reduced dimensionality quantum scattering calculation,<sup>47</sup> as well as a recent full dimensional ISSWP calculation<sup>49</sup> have been carried out for these reactions on the TSH3 PES. It is found that the thermal rate constant approximated by the rate constant for the ground initial state from the ISSWP approach<sup>49</sup> is significantly smaller than the experimental values in the low temperature region for the  $H_2 + CN$  reaction. Since the number of open rotational channels for this reaction is huge even at quite modest translational energy, owing to the tiny rotational constant of CN, it is obviously not feasible to use the ISSWP approach to obtain the rotationally averaged thermal rate constant. On the other hand, reactions such as this, which have a barrier and therefore a much lower density of states in the transition state region than the asymptotic region, are ideal for the TSWP approach.<sup>37</sup> We have used this approach to calculate the exact  $N(E)$  ( $J = 0$ ) on the TSH3 PES, from which the rate constants were computed by using the energy shifting approximation.

#### 3.1 The Hamiltonian and numerical parameters

The Hamiltonian for the diatom–diatom system in mass-scaled Jacobi coordinates can be written as<sup>38,52</sup>

$$H = \frac{1}{2\mu} \sum_{i=1}^3 \left( -\frac{\partial^2}{\partial s_i^2} + \frac{j_i^2}{s_i^2} \right) + V(s_1, s_2, s_3, \theta_1, \theta_2, \phi) \quad (9)$$

where  $j_2$  and  $j_3$  are the rotational angular momenta for  $H_2(D_2)$  and CN, which are then coupled to form  $j_{23}$ . In the body-fixed frame the orbital angular momentum,  $j_1$ , is represented as  $(J - j_{23})^2$ , where  $J$  is the total angular momentum. In eqn. (9),  $\mu$  is the

reduced mass of the system,

$$\mu = (M_1 M_2 M_3)^{1/3} \quad (10)$$

with  $M_i$  ( $i = 1-3$ ) being the reduced masses for the system,  $H_2(D_2)$  and CN, *i.e.*

$$M_1 = \frac{(m_H + m_H)(m_C + m_N)}{m_H + m_H + m_C + m_N},$$

$$M_2 = \frac{m_H m_H}{m_H + m_H},$$

$$M_3 = \frac{m_C m_N}{m_C + m_N}.$$

The mass-scaled coordinates  $s_i$  are defined as

$$s_i^2 = \frac{M_i}{\mu} R_i^2 \quad (11)$$

where  $R_i$  ( $i = 1-3$ ) are the intermolecular distance between the centers of mass of  $H_2$  and CN, and the bond lengths for  $H_2(D_2)$  and CN, respectively.

Now we define two new ‘reaction coordinate’ variables  $q_1$  and  $q_2$  by translating and rotating the  $s_1$  and  $s_2$  axes,<sup>37,53</sup>

$$\begin{pmatrix} q_1 \\ q_2 \end{pmatrix} = \begin{pmatrix} \cos \chi & \sin \chi \\ -\sin \chi & \cos \chi \end{pmatrix} \begin{pmatrix} s_1 - s_1^0 \\ s_2 - s_2^0 \end{pmatrix}. \quad (12)$$

It can be seen from this equation that we first move the origins of the  $(s_1, s_2)$  coordinates to  $(s_1^0, s_2^0)$ , then we rotate these two axes by the angle  $\chi$ . The new coordinates,  $q_1$  and  $q_2$  can now be defined as the ‘reaction coordinate’ and the ‘symmetric stretch coordinate’ for the collinear H–H–(CN) transition state.

The Hamiltonian in eqn. (9) can be written in term of  $q_i$  ( $i = 1, 2$ ) and  $s_3$  as

$$H = \frac{1}{2\mu} \left( -\sum_1^2 \frac{\partial^2}{\partial q_i^2} - \frac{\partial^2}{\partial s_3^2} + \sum_1^2 \frac{j_i^2}{s_i(q_1, q_2, s_1^0, s_2^0)^2} + \frac{j_3^2}{s_3^2} \right) + V \quad (13)$$

By choosing the dividing surface  $S_1$  at  $q_1 = 0$ , we can calculate the ‘internal’ transition states for the other five degrees of freedom by solving for the eigenstates of the 5-D Hamiltonian obtained by setting  $q_1 = 0$  in eqn. (13). After constructing the initial wavepackets in  $(q_1, q_2, s_3, \theta_1, \theta_2, \phi)$  coordinates, we transfer them to the  $(s_1, s_2, s_3, \theta_1, \theta_2, \phi)$  coordinates, and propagate them as in the regular wavepacket approach. The calculation of the bound states in 5-D has been presented in detail elsewhere,<sup>54</sup> and the propagation of the 6-D wavepacket in the diatom–diatom coordinates has also been shown;<sup>12</sup> thus we will not present them again here.

The parameters used in the current study are based on those employed in the initial state selected total reaction probability calculation carried out recently by Zhu *et al.*<sup>49</sup> We used a total number of 55 sine functions (among them 21 for the interaction region) for the translational coordinate  $s_1$  in a range of  $[3.5, 11.5]a_0$ . The number of vibrational basis functions used for the reagent CN is 2 or 3 depending on whether CN is vibrationally excited. A total of 19 and 22 vibrational functions are employed for  $s_2$  in the range of  $[0.3, 2.5]a_0$  for the reagents  $H_2$  and  $D_2$ , respectively. For the rotational basis, we used  $j_{3\max} = 41$  (for CN),  $j_{2\max} = 12$  for  $H_2$  and  $j_{2\max} = 16$  for  $D_2$ . The values of  $s_1^0, s_2^0$  and  $\chi$  that define the transition state surface were carefully chosen to be 5.1, 0.8 and  $47^\circ$  for  $H_2 + CN$ , and 5.5, 0.8 and  $48^\circ$  for  $D_2 + CN$ , to minimize the density-of-states on the

dividing surface. We propagated the TSWPs for 9000 au for the  $\text{H}_2 + \text{CN}$  reaction, and 10 500 au for the  $\text{D}_2 + \text{CN}$  reaction.

In addition to the separation of even and odd parities, which are related to the wave function symmetry with respect to torsion angle  $\phi = 0^{55}$  for the total angular momentum  $J = 0$ , the even and odd rotation states of  $\text{H}_2(\text{D}_2)$  can also be separated. In the present study, we only calculated the  $N(E)$  for the even rotation of  $\text{H}_2$ . Based on the fact that the transition state on the PES is quite rigid, we approximated the  $N(E)$  for the odd rotation of  $\text{H}_2(\text{D}_2)$  by that for the even rotation.

For the  $\text{H}_2 + \text{CN}$  reaction, we propagated 60 wavepackets (40 for even parity, 20 for odd parity) to converge the  $N(E)$  for energies up to 0.5 eV with respect to the ground rovibrational states of reagents. For the  $\text{D}_2 + \text{CN}$  reaction, we propagated 45 wavepackets (30 for even parity, 15 for odd parity) to converge the  $N(E)$  for energies up to 0.4 eV.

### 3.2 The cumulative reaction probability, $N(E)$ ( $J = 0$ )

We first show in Fig. 1 the number of open states of even parity as a function of energy in the asymptotic region and on the dividing surface  $S_1$  for the  $\text{H}_2 + \text{CN}$  reaction. Very obviously and importantly, the number of open states on  $S_1$  is much smaller than the number open in the asymptotic region. For  $E = 0.4$  eV, for example, the ratio between these is about 16. Thus for this reaction the TSWP should require many fewer wavepacket propagations in order to calculate  $N(E)$  than the ISSWP approach.

Fig. 2 shows the contributions of  $N_i(E)$  of different transition states to  $N(E)$  ( $i = 1-5, 10, 15, 20, 25, 30, 35$  for even parity). As can be seen from the figure, the  $N_i(E)$  for the first few states rise very quickly from 0 to about 1 in about 0.1 eV energy interval, then slightly decrease as the energy increases further. This rise in  $N_i(E)$  is significantly faster than that for the  $\text{H}_2 + \text{OH}$  reaction shown in Fig. 5 in ref. 38. This probably indicates that there is much less tunneling in the  $\text{H}_2 + \text{CN}$  reaction. Also we can see that the contributions to  $N(E)$  for the highly excited transition states are negligible for energy lower than 0.25 eV. The contributions to  $N(E)$  in that energy region almost all come from the first 4–5 transition states. For energy up to 0.5 eV, the first 40 wavepackets have already given very well converged  $N(E)$ . Among the  $N_i(E)$  shown in the figure, however, we can see the ‘non-probability’ nature of  $N_i(E)$ ; some have values slightly

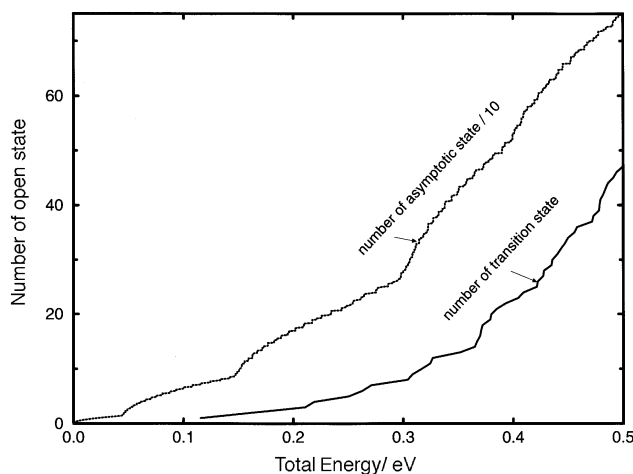


**Fig. 1** Number of open states as a function of total energy on transition state dividing surface and in asymptotic region divided by 10 for the  $\text{H}_2$  (even rotation) +  $\text{CN}$  reaction in even parity

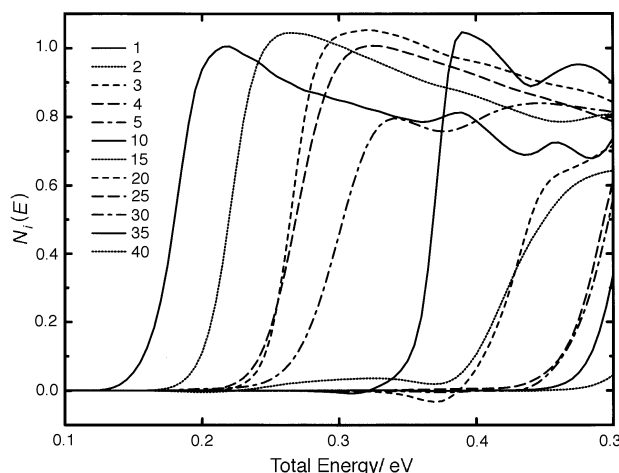


**Fig. 2** Some  $N_i(E)$ s ( $i = 1-5, 10, 15, 20, 25, 30, 35, 40$ ) as a function of total energy for the  $\text{H}_2$  (even rotation) + CN reaction in even parity

larger than 1, and some have very small negative contributions (a few percent) at some energies.

To our surprise, we found there are five out of the first 40 transition states that give rise to very strange oscillatory  $N_i(E)$  as shown in Fig. 3. Further investigation revealed that these five transition states correspond to the H—H—N—C configuration in the transition state region. These resonance-like structures in these  $N_i(E)$  are due to a deep well (close to 0.4 eV) along the reaction path in the H—H—N—C transition state region as shown in Fig. 4. Because the well is quite deep, the TSWPs initially located inside the well are resonantly trapped in the well, causing the oscillatory behavior in these  $N_i(E)$ . Since it is believed that the well is very likely unphysical, we just ignore these TSWPs. Thus the  $N(E)$  and later the rate constant presented in this paper are for the  $\text{H}_2 + \text{CN} \rightarrow \text{H—C—N} + \text{H}$  reaction.

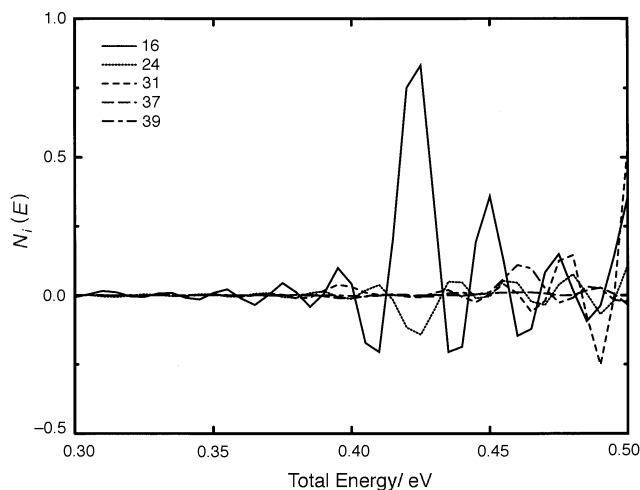


**Fig. 3** Oscillating  $N_i(E)$ s ( $i = 16, 24, 31, 37, 39$ ) for the H—H—N—C TSWPs as a function of total energy for the  $\text{H}_2$  (even rotation) + CN reaction in even parity

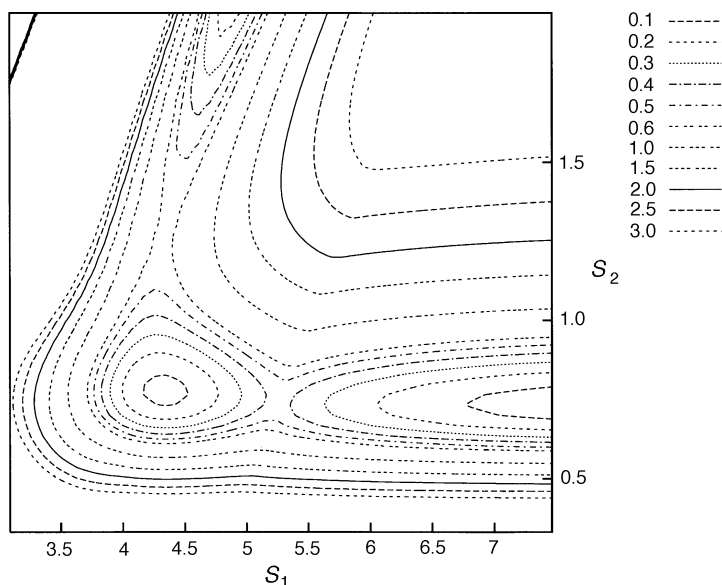


Fig. 4 PES for collinear H—H—N—C configuration with CN bond length optimized

The summation of  $N_i(E)$  for  $i = 1-40$  excluding those shown in Fig. 3 gives the  $N(E)$  for even parity shown in Fig. 5. The  $N(E)$  for odd parity shown in the figure are obtained in the same way. The total  $N(E)$  is simply the summation of  $N_i(E)$  for even and odd parities. From the figure, we can see that  $N(E)$  is very slightly oscillatory, not as smooth as that for the  $H_2 + OH$  reaction.<sup>38</sup> Fig. 6(b) shows the huge difference between  $N(E)$  for  $H_2 + CN$  and  $H_2 + OH$  in the low-energy region. The  $N(E)$  for the  $H_2 + CN$  reaction is much smaller than that for the  $H_2 + OH$  reaction for energy lower than 0.14 eV. This implies the tunneling effect in the  $H_2 + OH$  reaction is much more significant than that in the  $H_2 + CN$  reaction.

The  $N(E)$  for the  $D_2 + CN$  reaction for energies up to 0.4 eV is shown in Fig. 6 together with that for the  $H_2 + CN$  reaction. First, we can see the  $N(E)$  curve for the  $D_2 + CN$  reaction also shows slight oscillatory behavior, like that for the  $H_2 + CN$  reaction. For energy higher than 0.16 eV, the  $N(E)$  for the  $D_2 + CN$  reaction is higher than that for the  $H_2 + CN$  reaction because of the larger density-of-states for  $D_2 + CN$  in the transition state region. For energies lower than about 0.16 eV, where tunneling effects are dominant, the  $N(E)$  for the  $D_2 + CN$  reaction becomes smaller than that for the  $H_2 + CN$  reaction because of the heavier mass of the D atoms.

### 3.3 Thermal rate constants

The thermal rate constant can be calculated from the cumulative reaction probability via a Boltzmann average,

$$k(T) = [2\pi Q_r(T)]^{-1} \int_{-\infty}^{+\infty} dE e^{-E/k_B T} N_{\text{tot}}(E) \quad (14)$$

where  $Q_r(T)$  is the reactant partition function (per unit volume),  $N_{\text{tot}}(E)$  is the total cumulative reaction probability,

$$N_{\text{tot}}(E) = \sum_J (2J + 1) N_J(E) \quad (15)$$

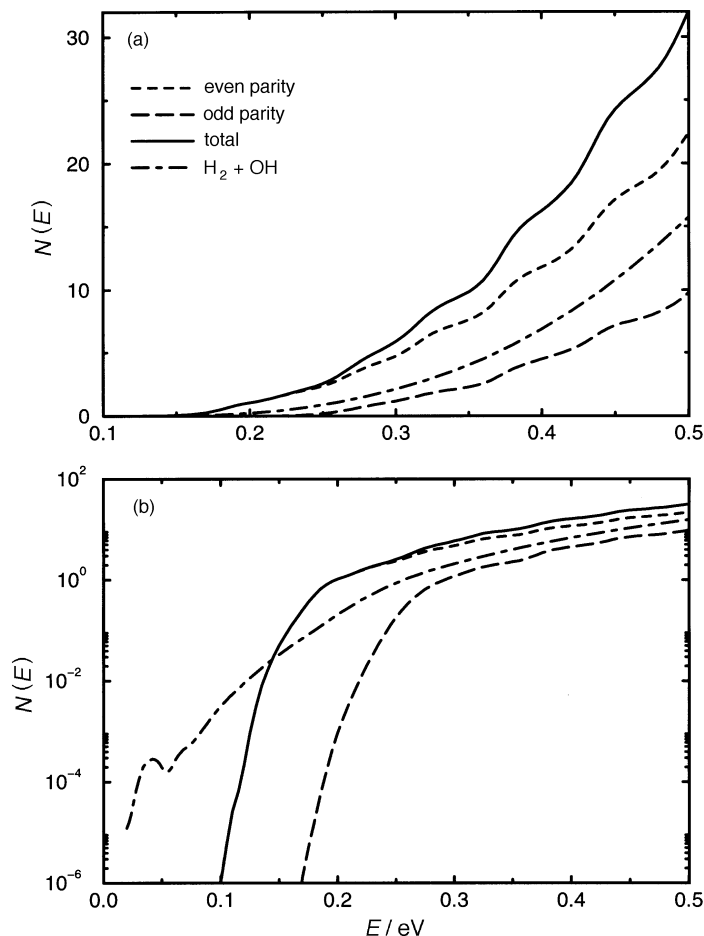


**Fig. 5** Cumulative reaction probability  $N(E)$  as a function of total energy for the  $H_2$  (even rotation) +  $CN \rightarrow HCN + H$  reaction, compared with that for the  $H_2$  (even rotation) +  $OH$  reaction: (a) linear scale; (b) logarithmic scale

with  $J$  being the total angular momentum. Since the calculation of the  $N_{J=0}(E)$  alone takes more than 1 month of CPU time on an SGI R10000 processor, it is obviously not feasible to calculate the total cumulative reaction probability by using the same method with our current computer power. Thus we invoke the energy shifting approximation to calculate the approximate rate constant from the exact  $N_{J=0}(E)$ . Since the reaction has a linear transition state, the approximate rate constant should be calculated as<sup>56,57</sup>

$$k_{\text{energy shifting}}(E) \approx \frac{Q_{\text{rot}}^{\ddagger} C^{\ddagger}}{2\pi Q_r(T)} \int_{-\infty}^{\infty} dE e^{-E/k_B T} N_{J=0}(E) \quad (16)$$

where  $Q_{\text{rot}}^{\ddagger}$  is the rotational partition function for the linear  $H_2CN(D_2CN)$  complex at the (transition state) saddle point and can be easily calculated as

$$Q_{\text{rot}}^{\ddagger} = \sum_J (2J + 1) \exp(-E_{\text{rot}}^J/k_B T) \quad \text{with} \quad E_{\text{rot}}^J = B_{\text{rot}}^{\ddagger} J(J + 1) \quad (17)$$

where  $B_{\text{rot}}^{\ddagger}$  is the rotational constant of the linear reaction complex at the saddle point; it is  $0.757 \text{ cm}^{-1}$  for the  $H_2CN$  complex and  $0.495 \text{ cm}^{-1}$  for the  $D_2CN$  complex.  $C^{\ddagger}$  in eqn.

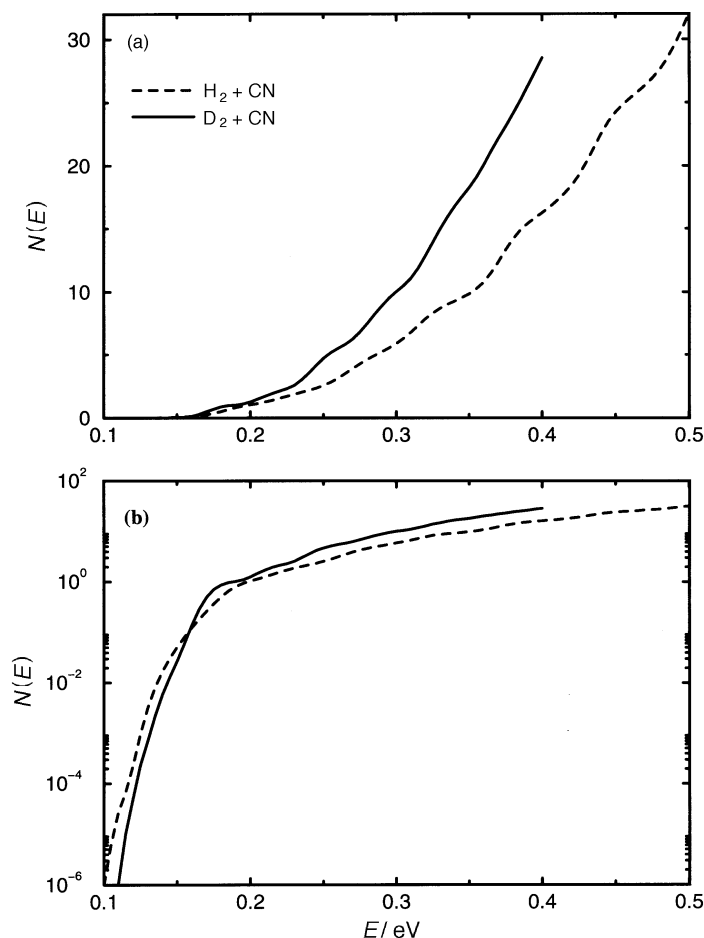


**Fig. 6** Comparison of  $N(E)$  for the  $\text{H}_2$  (even rotation) + CN reaction and the  $\text{D}_2$  (even rotation) + CN reaction: (a) linear scale; (b) logarithmic scale

(16) is a kind of bending partition function of a linear (doubly degenerate) transition state. For a linear four atom system, there are two doubly degenerate bending states and  $C^\ddagger$  can be calculated as<sup>56</sup>

$$C^\ddagger = 1 + \frac{2 \exp(-\hbar\omega_1^\ddagger/k_{\text{B}}T)}{1 - \exp(-\hbar\omega_1^\ddagger/k_{\text{B}}T)} + \frac{2 \exp(-\hbar\omega_2^\ddagger/k_{\text{B}}T)}{1 - \exp(-\hbar\omega_2^\ddagger/k_{\text{B}}T)}. \quad (18)$$

For the  $\text{H}_2\text{CN}$  complex,  $\omega_1^\ddagger$  and  $\omega_2^\ddagger$  are  $114.6 \text{ cm}^{-1}$  and  $562.3 \text{ cm}^{-1}$ , respectively. For the  $\text{D}_2\text{CN}$  complex,  $\omega_1^\ddagger$  and  $\omega_2^\ddagger$  are  $103.5 \text{ cm}^{-1}$  and  $398.62 \text{ cm}^{-1}$ , respectively.

The rate constants calculated using eqn. (16) are shown in Fig. 7 for temperatures between 200 and 750 K for the  $\text{H}_2 + \text{CN}$  reaction and for temperatures between 200 and 600 K for the  $\text{D}_2 + \text{CN}$  reaction. Also shown in Fig. 7 are the experimental rate constants for these two reactions.<sup>43,45</sup> For the  $\text{H}_2 + \text{CN}$  reaction, the agreement between the theory and experiment is only good in the high-temperature region. As the temperature decreases, the experimental value becomes increasingly larger than the theoretical one. At  $T = 209 \text{ K}$ , the experimental value is larger than the theoretical one by a factor of 2.4. For the  $\text{D}_2 + \text{CN}$  reaction the theoretical rate constants agree quite well with all the available experimental data. However, because there is no experimental value measured at  $T = 209 \text{ K}$ , it is very hard to say if the theory can agree with experi-

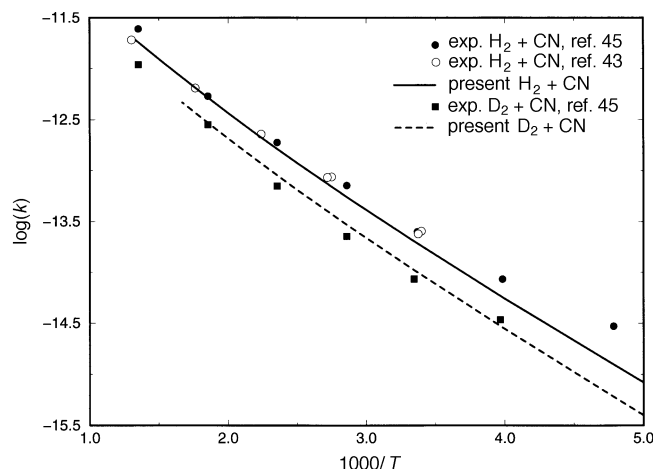


**Fig. 7** Comparison of the present theoretical rate constant with the experimental measurements for the  $\text{H}_2(\text{D}_2) + \text{CN}$  reaction

ment at that low temperature. We also should bear in mind that we invoked the energy shifting approximation to calculate these rate constants from  $N(E)$  ( $J = 0$ ). The accuracy of this approximation for these two reactions still must be assessed. Meanwhile if we assume that the energy shifting approximation is quite good for these two reactions, then the comparison between theoretical and experimental results indicates that the tunneling effect is not significant enough on the TSH3 PES.

We also compare the present rate constant with other theoretical results on the same PES in Fig. 8. In the high-temperature region, all the calculations agree with each other quite well. Over the whole temperature region, the rate constants for the ground initial state agree very well with our results. In the low-temperature region, the present value is slightly higher than that for the ground initial state (at  $T = 200$  K, the present value is higher than that for the ground initial state by 16%). In the high-temperature region, the rate constant for the ground initial state is slightly higher than the present value (at  $T = 700$  K, the rate constant for the ground initial state is higher than the present value

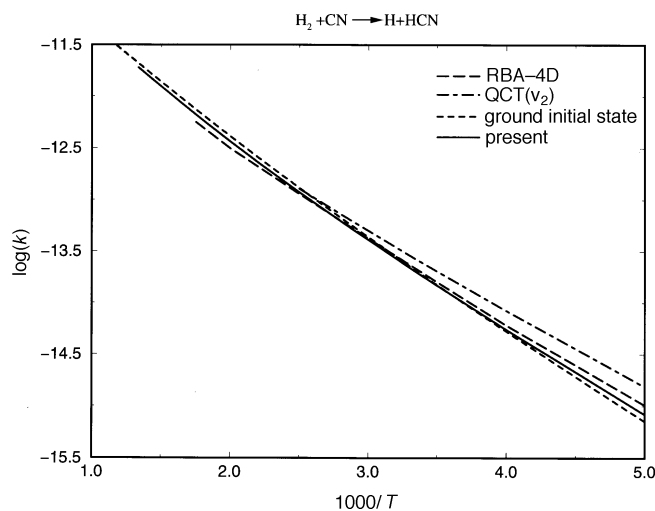


**Fig. 8** Comparison of the present theoretical rate constant with other theoretical results for the  $\text{H}_2 + \text{CN}$  reaction

by 10%). It is worth pointing out that the approximation of the thermal rate constant by that for the ground initial state neglects the reagent rotational effect on rate constants, whereas it treats the high  $J$  effect by the CS approximation. On the other hand, the effects from initial reagent rotation are treated accurately in the current study, while the high  $J$  effect is treated quite crudely by the energy shifting approximation. Realizing the essential difference in the approximations made in these two calculations, it is quite interesting to see such good agreement between them. It is found in a recent study of the  $\text{H}_2 + \text{OH}$  reaction<sup>39</sup> that in the high-temperature region the rate constant for the ground initial state is slightly higher than the accurate value, whereas in the low-temperature region the rate constant for the ground initial state is slightly lower than the accurate result. If this is also true for the  $\text{H}_2 + \text{CN}$  reaction, this would mean that the rate constant from the energy shifting approximation is quite accurate.

Finally, we can see that in the low-temperature region the RB (rotating bond) 4-D results<sup>47</sup> are slightly higher than the current results, whereas the rate constants obtained from quasiclassical trajectory calculations, which agree very well with the experimental results, are significantly larger than the current values.

The role of the metastable well in the HHNC configuration on the TSH3 PES has not been examined as the well might be an artifact. Hence the current results exclude transition states located in this well. However, if the  $N_i(E)$  from these transition states were included, the effect on the overall rate constants would be small. The sum of  $N_i(E)$  from these states is less than 0.1 for energies below 0.40 eV, and remains between about  $-0.2$  and  $+0.6$  for energies between 0.40 eV and 0.5 eV. At energies above 0.4 eV the  $N(E)$  from the ‘true’ transition states is larger than 15. Thus the contribution from the metastable states, real or not, is not significant. It also should be noted that the reaction probability from these HHNC configurations might result in formation of the HNC isomer. The current dividing surface lumps the two isomers as ‘product’ since it does not depend on the polar angle of CN with respect to the intermolecular axis. It will be interesting to investigate this possibility in the future.

## 4 Conclusions

We have evaluated the cumulative reaction probability for the reaction of  $\text{H}_2(\text{D}_2)$  with CN for  $J = 0$  by the TSWP method. We find that the method is highly advantageous for this system because of the relatively high barrier and low density-of-states in the transition state region. The cumulative reaction probability is a smooth function of energy except for contributions from (possibly spurious) transition states located in the metastable HHNC minimum. The thermal rate constants are approximated from  $N(E)$  for  $J = 0$  by the energy shifting approximation. Surprisingly good agreement is obtained between this calculation and two earlier calculations, the first based on a 4-D RB approximation,<sup>47</sup> and the second an exact quantum initial state selected calculation for the ground state system (with initially non-rotating  $\text{H}_2$  and CN). However, all three quantum calculations are not in good agreement with experiment or with quasiclassical calculations at low temperatures. This suggests (but certainly doesn’t prove) that the PES might not permit enough tunneling and/or that the zero point energies at the transition state are too large. The agreement with experiment at higher temperatures for both  $\text{H}_2 + \text{CN}$  and  $\text{D}_2 + \text{CN}$  is excellent.

This research was supported in part by a grant from the Department of Energy, DE-F602-87ER 13679, and by Academic research grant RP970632, National University of Singapore.

## References

- 1 E. Wigner, *J. Chem. Phys.*, 1937, **5**, 720.
- 2 S. Glasston, K. J. Laidler and H. Eyring, *The Theory of Rate Processes*, McGraw-Hill, New York, 1941.

- 3 J. C. Keck, *J. Chem. Phys.*, 1960, **32**, 1035.
- 4 J. C. Keck, *Adv. Chem. Phys.*, 1967, **13**, 85.
- 5 P. Pechukas and F. J. McLafferty, *J. Chem. Phys.*, 1973, **58**, 1622.
- 6 P. Pechukas, *Modern Theoretical Chemistry*, ed. W. H. Miller, Plenum, New York, Part B, vol. 2, 1976.
- 7 B. C. Garrett and D. G. Truhlar, *J. Chem. Phys.*, 1979, **70**, 1593.
- 8 D. G. Truhlar and B. C. Garrett, *Annu. Rev. Phys. Chem.*, 1984, **35**, 159.
- 9 D. G. Truhlar, B. C. Garrett and S. J. Klippenstein, *J. Phys. Chem.*, 1996, **100**, 12771.
- 10 D. H. Zhang and J. Z. H. Zhang, *J. Chem. Phys.*, 1993, **99**, 5615.
- 11 D. Neuhauser, *J. Chem. Phys.*, 1994, **100**, 9272.
- 12 D. H. Zhang and J. Z. H. Zhang, *J. Chem. Phys.*, 1994, **101**, 1146.
- 13 D. H. Zhang and J. C. Light, *J. Chem. Phys.*, 1996, **104**, 4544.
- 14 D. H. Zhang and J. C. Light, *J. Chem. Phys.*, 1996, **105**, 1291.
- 15 W. Zhu, J. Dai, J. Z. H. Zhang and D. H. Zhang, *J. Chem. Phys.*, 1996, **105**, 4881.
- 16 W. H. Miller, *J. Chem. Phys.*, 1974, **61**, 1823.
- 17 W. H. Miller, S. D. Schwartz and J. W. Tromp, *J. Chem. Phys.*, 1983, **79**, 4889.
- 18 J. W. Tromp and W. H. Miller, *Faraday Discuss. Chem. Soc.*, 1987, **84**, 441.
- 19 K. Yamashita and W. H. Miller, *J. Chem. Phys.*, 1985, **82**, 5475.
- 20 J. W. Tromp and W. H. Miller, *J. Phys. Chem.*, 1986, **90**, 3482.
- 21 T. P. Park and J. C. Light, *J. Chem. Phys.*, 1986, **85**, 5870.
- 22 T. P. Park and J. C. Light, *J. Chem. Phys.*, 1988, **88**, 4897.
- 23 T. P. Park and J. C. Light, *J. Chem. Phys.*, 1989, **91**, 974.
- 24 T. P. Park and J. C. Light, *J. Chem. Phys.*, 1991, **94**, 2946.
- 25 D. Brown and J. C. Light, *J. Chem. Phys.*, 1992, **97**, 5465.
- 26 W. H. Thompson and W. H. Miller, *J. Chem. Phys.*, 1995, **102**, 7409.
- 27 W. H. Thompson and W. H. Miller, *J. Chem. Phys.*, 1994, **101**, 8620.
- 28 (a) P. Day and D. Truhlar, *J. Chem. Phys.*, 1991, **94**, 2045; (b) P. Day and D. Truhlar, *J. Chem. Phys.*, 1991, **95**, 5097; (c) D. Neuhauser and M. Baer, *J. Chem. Phys.*, 1989, **90**, 4351.
- 29 U. Manthe and W. H. Miller, *J. Chem. Phys.*, 1993, **99**, 3411.
- 30 U. Manthe, T. Seideman and W. H. Miller, *J. Chem. Phys.*, 1993, **99**, 10078.
- 31 U. Manthe, T. Seideman and W. H. Miller, *J. Chem. Phys.*, 1994, **101**, 4759.
- 32 U. Manthe, *J. Chem. Phys.*, 1995, **102**, 9204.
- 33 W. H. Thompson and W. H. Miller, *J. Chem. Phys.*, 1997, **106**, 142.
- 34 H. Wang, W. H. Thompson and W. H. Miller, *J. Chem. Phys.*, 1997, **107**, 7194.
- 35 U. Manthe and F. Matzkies, *Chem. Phys. Lett.*, 1996, **252**, 7.
- 36 (a) F. Matzkies and U. Manthe, *J. Chem. Phys.*, 1997, **106**, 2646; (b) U. Manthe and F. Matzkies, *Chem. Phys. Lett.*, 1998, **282**, 442; (c) F. Matzkies and U. Manthe, *J. Chem. Phys.*, 1998, **108**, 4828.
- 37 D. H. Zhang and J. C. Light, *J. Chem. Phys.*, 1996, **104**, 6184.
- 38 D. H. Zhang and J. C. Light, *J. Chem. Phys.*, 1997, **106**, 551.
- 39 D. H. Zhang, J. C. Light and S. Y. Lee, *J. Chem. Phys.*, 1998, **109**, 79.
- 40 B. Jackson, *Annu. Rev. Phys. Chem.*, 1995, **46**, 251.
- 41 D. H. Zhang and J. Z. H. Zhang, in *Dynamics of molecules and chemical reactions*, ed. R. E. Wyatt and J. Z. H. Zhang, Marcel Dekker, New York, 1996.
- 42 T. Seideman and W. H. Miller, *J. Chem. Phys.*, 1991, **95**, 1768.
- 43 I. R. Sims and I. W. M. Smith, *Chem. Phys. Lett.*, 1988, **149**, 564.
- 44 Q. Sun and J. M. Bowman, *J. Chem. Phys.*, 1990, **92**, 5201.
- 45 Q. Sun, D. L. Yan, N. S. Wang, J. M. Bowman and M. C. Lin, *J. Chem. Phys.*, 1990, **93**, 4730.
- 46 M. A. ter Horst, G. c. Schatz and L. B. Harding, *J. Chem. Phys.*, 1996, **105**, 2309.
- 47 T. Takayanagi and G. C. Schatz, *J. Chem. Phys.*, 1997, **106**, 3227.
- 48 J. H. Wang, K. Liu, G. C. Schatz and M. ter Horst, *J. Chem. Phys.*, 1997, **107**, 7869.
- 49 W. Zhu, J. Z. H. Zhang, Y. C. Zhang, Y. B. Zhang, L. X. Zhang and S. L. Zhang, *J. Chem. Phys.*, 1998, **108**, 3509.
- 50 L.-H. Lai, J.-H. Wang, D. C. Che and K. Liu, *J. Chem. Phys.*, 1996, **105**, 3332.
- 51 J. M. Bowman and G. C. Schatz, *Annu. Rev. Phys. Chem.*, 1995, **46**, 169.
- 52 D. C. Clary, *J. Chem. Phys.*, 1991, **95**, 7298.
- 53 J. M. Bowman, J. Zuniga and A. Wierzbicki, *J. Chem. Phys.*, 1989, **90**, 2708.
- 54 D. H. Zhang, Q. Wu, J. Z. H. Zhang, M. Dirke and Z. Bačić, *J. Chem. Phys.*, 1995, **102**, 2315.
- 55 D. H. Zhang and J. Z. H. Zhang, *J. Chem. Phys.*, 1994, **100**, 2697.
- 56 Q. Sun, J. M. Bowman, G. C. Schatz, J. R. Sharp and J. N. L. Connor, *J. Chem. Phys.*, 1990, **92**, 1677.
- 57 J. M. Bowman, *J. Phys. Chem.*, 1991, **95**, 4960.